

# Non-linear elasticity of a liquid contact line

A. CHECCO<sup>(a)</sup>

*Condensed Matter Physics and Materials Science Department, Brookhaven National Laboratory  
Upton, NY 11973, USA*

received 21 October 2008; accepted in final form 5 December 2008  
published online 19 January 2009

PACS 68.08.Bc – Wetting

PACS 68.03.Cd – Surface tension and related phenomena

**Abstract** – By using energy minimization computations we study the distortion of a wetting contact line pinned on a single defect. We find that the elastic restoring force of the line depends non-linearly on the amplitude of the distortion and we estimate the anharmonic corrections to the linear elastic model. These results suggest the importance of non-linear effects in the problem of contact line pinning.

Copyright © EPLA, 2009

**Introduction.** – “Partial wetting” refers to a situation when solid, liquid and gas phases coexist along the so-called “contact line” (CL). A deformation of the CL from its equilibrium shape causes a long-range distortion of the liquid/gas interface which results in a non-local elasticity [1]. CL distortions occur naturally when a liquid wets partially a heterogeneous solid in which case the CL is pinned on the local changes in substrate wettability or “defects”. The phenomenon of CL pinning is relevant to a large number of applications including water repellency [2], coating and printing technologies and the mediated self-assembly of nano-objects [3].

CL elasticity has been modeled using the linear approximation firstly introduced by Joanny and de Gennes (JdG) [4]. Within this approximation, strictly valid in the limit of small CL deformations, the restoring force of the CL has the linear, non-local form

$$F_{el}[\eta] = \frac{\gamma \sin^2 \theta}{\pi} \int \frac{\eta(x')}{(x - x')^2} dx', \quad (1)$$

where  $\eta(x')$  is the normal displacement of the CL from its average position at the coordinate  $x'$  along the line,  $x$  is the coordinate of the force pinning the line,  $\gamma$  is the liquid surface tension and  $\theta$  the contact angle of the liquid on the substrate.

However, recent experiments [5] have found that the roughness of a portion  $\ell$  of the CL on a heterogeneous surface scales as  $\ell^\zeta$  with an exponent  $\zeta \approx 1/2$ , sensibly larger than predicted by the linear JdG model [6]. This discrepancy has risen the question whether linear elasticity can accurately describe the stiffness of a real CL.

Le Doussal *et al.* [7] have recently shown that a large enough second-order correction to eq. (1) may increase the theoretical roughness exponent thus reducing the discrepancy between theory and experiment. Although this result is suggestive of the importance of non-linear effects, a quantitative analysis of the non-linear elasticity of the CL is still lacking.

In this paper we use energy minimization calculations to determine the equilibrium configurations of a CL pinned on an isolated defect and the associated restoring force. We find that the computed force is in excellent quantitative agreement with the linear approximation only for distortions significantly smaller than the characteristic size of the defect. Beyond this limit, the force depends non-linearly on the amplitude of the distortion and we estimate the anharmonic coefficients of the CL stiffness. These results suggest the importance of non-linear effects in the problem of CL pinning and may lead to refined theoretical models of CL elasticity.

**Numerical methods.** – Similarly to JdG’s approach [4] we approximate the shape of the unperturbed fluid surface near the CL as an inclined plane making a contact angle  $\bar{\theta}$  with the solid as illustrated in fig. 1(a). This assumption is valid at length scales smaller than the *capillary length*  $\kappa^{-1} = (\gamma/\rho g)^{1/2}$  and when the fluid is connected to an infinite reservoir. Here we are interested in the case of a flat homogeneous solid that exhibits a single, squared defect of size  $\xi$  centered at the coordinates  $(x_d, y_d)$ . The wettability of the defect is a function  $\theta(x, y)$  of the substrate coordinates  $(x, y)$ . The surface free energy of a finite portion of the liquid wedge

<sup>(a)</sup>E-mail: checco@bnl.gov

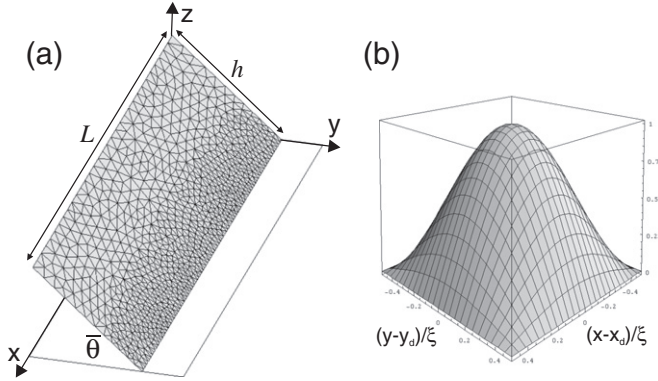


Fig. 1: (a) The shape of the unperturbed liquid surface near the CL is approximated by an inclined plane, surface area  $L \times h$ , making a contact angle  $\bar{\theta}$  with the solid. The liquid surface is represented by a piecewise linear set of  $N$  triangular facets. (b) The wettability of an isolated defect in the case  $\bar{\theta} = 90^\circ$ .

pinned on the defect can be written as

$$G = \gamma_{lg}\Sigma_{lg} - \gamma_{lg} \int_{\Sigma_{sl}} \cos \theta(x, y) dx dy, \quad (2)$$

where  $\Sigma_{lg}$  and  $\Sigma_{sl}$  are the portions of the liquid wedge in contact with the gas and the solid respectively.

Here we model the defect wettability with the following function:

$$\cos \theta(x, y) = \cos \bar{\theta} + (1 - \cos \bar{\theta}) \cos \pi \frac{(x - x_d)}{\xi} \cos \pi \frac{(y - y_d)}{\xi}. \quad (3)$$

This specific defect “structure”, shown in fig. 1(b), exhibits non-smooth boundaries and a center which is completely wet by the liquid (“attractive” defect). Although other defect structures can be considered, the results of this paper only depend quantitatively on this particular choice. For example, a defect with sharper edges would pin more strongly the CL resulting in a stronger restoring force. However, the qualitative behavior of this force is independent of the “strength” of the defect.

Once the functional form of the heterogeneity  $\cos \theta(x, y)$  is defined, minimization of the free energy  $G$  with respect to  $\Sigma_{lg}$ , under the constraint of constant wedge’s volume, provides the equilibrium shape of the liquid-gas interface and in particular of the CL. We have performed this minimization numerically making use of the public-domain software “Surface Evolver” (SE) [8,9]. This package has been already used to study equilibrium liquid morphologies on chemically patterned surfaces [10,11] or on substrates with spatially periodic wettability [12]. To our knowledge, this is the first application to the study of CL pinning.

To minimize the system free energy, eq. (2), using the SE the liquid-gas interface is represented by a piecewise linear set of  $N$  triangular facets each one supporting three vertices at its corners. The initial configuration of the

facets is a finite portion of a plane, length  $L$ , making an angle  $\bar{\theta}$  with the solid as illustrated in fig. 1(a).  $L/2$  sets a lateral cut-off scale of the interface distortion which in an actual experiment can be identified with  $\kappa^{-1}$  or a macroscopic sample size. In order to increase the accuracy yet reduce the computing time, the facet density is increased in the vicinity of the CL where the interface distortion is expected to be larger. Vertices and facets lying on the  $(x, z)$ -plane are deemed on a horizontal line, which sets the boundary condition of planar interface sufficiently far away from the CL (constraint  $C_h$ ). This is equivalent to introducing a cut-off length  $h$  of the interface distortion in the vertical coordinate. We have set  $L \simeq h \gg \xi$  to ensure accurate results. Vertices initially lying on the planes  $(x, y, 0)$  (*i.e.* the  $n$  points belonging to the CL),  $(0, y, z)$  and  $(L, y, z)$  are constrained to these surfaces. All other vertices are free to move in every direction. Under these constraints the first term on the right side of eq. (2) is calculated by the SE as the total area of the facets. The second term is computed not as a surface but as a line integral along the CL using the Stoke’s theorem [9]. Starting from the initial configuration of fig. 1(a) the equilibrium shape of the liquid free surface is obtained by the SE in an iterative manner using a gradient descent technique.

**Results and discussion.** – We have calculated the equilibrium distortion induced by the defect pictured in fig. 1(b) on a portion  $L$  of the CL for small, intermediate and large contact angles, respectively  $\bar{\theta} = 10^\circ, 45^\circ$  and  $90^\circ$ . For these specific computations we have used the parameters  $N = 4700, n = 150, L/\xi = 50$  and  $h = L$  with the defect positioned at the reduced coordinate  $(x/\xi = 25, y/\xi = 25)$ . The choice of the ratio  $L/\xi$  is consistent to the experiments [5,13] where typically  $L \simeq 1$  mm and  $\xi \simeq 10$   $\mu$ m. The wedge is retracted progressively until the defect, initially buried under the liquid, pins the CL. To retract the wedge we translate the coordinate  $y_h$  of the constraint  $C_h$  by a small amount  $\Delta y_h/\xi = -2.5 \times 10^{-2}$  and we re-evolve the surface to the energy minimum  $\hat{G}(y_h)$  within the machine precision (15 digits). This precise minimization ensures the high accuracy of the force computation. The equilibrium configurations of the pinned CL,  $\eta(x)$ , are shown in fig. 2(a) for a contact angle  $\bar{\theta} = 45^\circ$ . These curves illustrate (from top to bottom) the progressive distortion of the CL as it moves across the defect. The CL is not perfectly pinned at the defect boundaries because the defect exhibits relatively smooth edges. The amplitude of the CL distortion, defined as  $\eta_M = \eta(x/\xi = 25) - \eta(x/\xi = 50)$ , increases reaching the maximum  $\eta_M = 0.75\xi$ . Subsequently, the CL detaches from the defect relaxing to its unperturbed shape (not shown).

To test the accuracy of the linear model we have compared the numerical CL shape to the logarithmic JdG profile [4]  $\eta(x) = F_0 \ln(L_c/|x - d|)$ . For this purpose, a logarithmic function (solid line) was fitted to the numerical profile (open dots) omitting data points close to the defect  $|x/\xi - 25| < 1/4$  as illustrated in fig. 2(b).

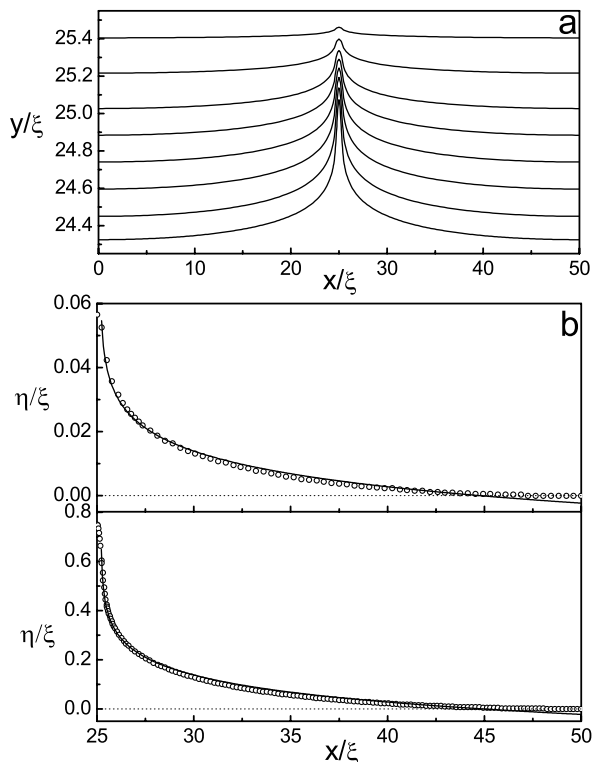


Fig. 2: (a) Equilibrium configurations of a CL that is progressively retracted across a wettable defect for  $\bar{\theta} = 45^\circ$ . (b) Logarithmic fits (solid lines) to the CL configurations (open dots) for small ( $\eta_M = 0.056\xi$ , top) and large ( $\eta_M = 0.75\xi$ , bottom) distortions.

For both small ( $\eta_M = 0.056\xi$ , top) and large ( $\eta_M = 0.75\xi$ , bottom) distortions the logarithmic shape describes reasonably well the numerical profile with the best-fit parameters  $d = 0.2\xi$  and  $L_c = 19.7\xi$ .  $d$  represents the effective radius of the defect which, as expected, is smaller than  $\xi/2$  because the defect exhibits smooth edges. The goodness of the fit (as indicated by the  $\chi^2$  values) is better for small distortions and in general the logarithmic profile does not describe very accurately the CL shape far from the defect because the fitted  $L_c$  is smaller than the characteristic cut-off length of the system,  $L/2 = 25\xi$ . This means that the simulated CL profile decays to the unperturbed position more rapidly than a logarithmic fall-off. These findings are consistent to the experiment by Nadkarni and Garoff [13] who have studied the shape of the CL pinned on a single defect. These authors have also found that the values of  $L_c$  obtained from fits to the experimental CL profiles were sensibly smaller than the expected cut-off length set by gravitational forces. They have attributed this discrepancy to the effect of substrate inhomogeneity that interferes with the gravitational flattening of the CL. However, our results show that this discrepancy may result not only from the inhomogeneity of the solid but also from the inaccuracy of the logarithmic profile to model the decay of the CL distortion.

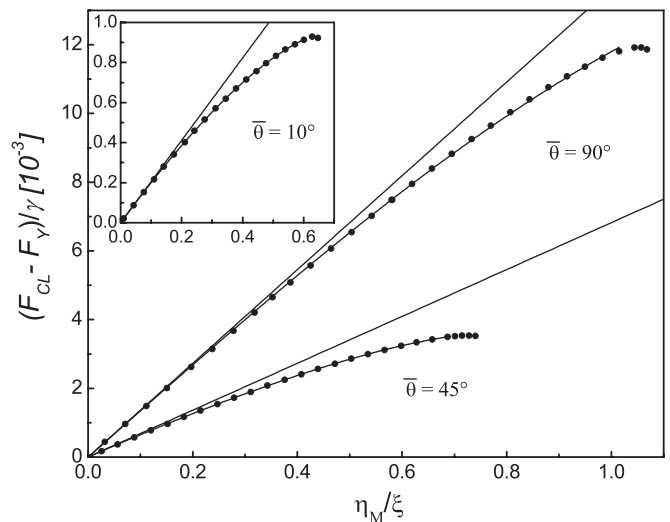


Fig. 3: (a) Reduced force per unit length of the CL (dots) plotted as a function of  $\eta_M$  for  $\bar{\theta} = 10^\circ$  (inset),  $45^\circ$  and  $90^\circ$ . Lines represent the linear JdG force whereas curves are polynomial fits to the data excluding points close to the depinning threshold.

For each value of  $\eta_M$  we have calculated the reduced restoring force per unit length of the CL by using the Finite Differences method

$$\frac{F_{CL}(y_h, \eta_M)}{\gamma} = \frac{\hat{G}(y_h + \delta y_h) - \hat{G}(y_h - \delta y_h)}{2\delta y_h L}, \quad (4)$$

where  $\hat{G}(y_h \pm \delta y_h)$  are the energy minima computed after the wedge has been translated, respectively, along the direction  $\pm y$  by a small amount  $\delta y_h/\xi = -2.5 \times 10^{-6}$ . The value of  $\delta y_h$  was chosen in order to achieve a  $10^{-7}$  accuracy in the force computation.

The reduced force per unit length of the CL (minus the reduced Young force  $F_Y/\gamma = \cos\theta$ ) is plotted as a function of the reduced distortion  $\eta_M/\xi$  for  $\theta = 10^\circ$  (inset),  $45^\circ$  and  $90^\circ$  in fig. 3. The results indicate that, for each value of  $\bar{\theta}$ , the restoring force scales linearly with  $\eta_M$  only for small values of the distortion ( $\eta_M/\xi \leq 0.1$ ). In this linear regime the computed force is in excellent quantitative agreement with eq. (1) using  $d$  and  $L_c$  (as obtained from the logarithmic fits) as lower and upper cutoff lengths respectively:  $\frac{F_{JdG}}{\gamma} = \left[ \frac{\pi\xi \sin^2 \bar{\theta}}{L \ln(L_c/d)} \right] \eta_M/\xi$  (lines). The coefficient in the square brackets is the JdG “spring constant” of the line. This result proves the reliability and accuracy of the numerical computations. For larger distortions, the restoring force increases non-linearly with an apparent “softening” until saturation occurs in proximity of the depinning threshold. Close to the depinning, because of non-linear effects, the JdG approximation overestimates the actual value of the reduced force by 43% for  $\bar{\theta} = 10^\circ$  and 20% for  $\bar{\theta} = 90^\circ$ .

Table 1: Coefficients  $k_i$  of a 4th-order power series expansion of the contact line force along with values of  $k_{JdG}$  for various  $\bar{\theta}$ 's.

$\theta$	$10^\circ$	$45^\circ$	$90^\circ$
$k_{JdG} (10^{-3})$	2.1	6.8	13.6
$k_1 (10^{-3})$	$2.1 \pm 0.1$	$6.7 \pm 0.1$	$13.5 \pm 0.1$
$k_2 (10^{-3})$	$-0.8 \pm 0.1$	$-2.3 \pm 0.2$	0
$k_3 (10^{-3})$	$0.1 \pm 0.2$	$2.0 \pm 0.5$	$-1.7 \pm 0.1$
$k_4 (10^{-3})$	$-0.6 \pm 0.2$	$-3.2 \pm 0.3$	0

We have expressed the non-linearity of the CL force in terms of a power series of order  $n$ :

$$\frac{F_{CL} - F_Y}{\gamma} = \sum_{i=1}^n k_i (\eta_M / \xi)^i, \quad (5)$$

where  $k_i$  represents the coefficient of the  $i$ -th term. Coefficients up to the 4th order have been estimated by fitting eq. (5) (with  $n = 4$ ) to the numerical force data. For  $\bar{\theta} = 90^\circ$  only odd indices have been retained to account for the symmetry of the CL energy upon the inversion  $\eta \rightarrow -\eta$  [7]. Results of this calculations are summarized in table 1 along with the values of  $k_{JdG}$  for various  $\bar{\theta}$ 's. There is an excellent agreement between  $k_1$  and  $k_{JdG}$  for every  $\bar{\theta}$  indicating that, as expected, the linear model is accurate for small perturbations. The second-order coefficients are always negative for  $\bar{\theta} \neq 90^\circ$  which reflects the softening of the restoring force at large distortions. This also occurs for  $\bar{\theta} = 90^\circ$  since in this case the third-order coefficient is negative. The magnitude of the anharmonic coefficients relative to the harmonic term decreases with  $\bar{\theta}$  suggesting that the non-linearity of the CL elasticity decreases with the stiffness of the line (which is proportional to  $\sin^2 \bar{\theta}$  in first approximation). However, non-linear effects are significant for all the values of  $\bar{\theta}$  studied here.

Although the results described above were obtained for a specific defect's energy, the CL elasticity exhibits a similar non-linear behavior regardless of the specifics of the defect's energy. This is suggested by similar calculations performed using a defect with a larger pinning strength. In this case, for the same  $\eta_M$  and  $\bar{\theta}$ , the restoring force of the line is found to be slightly larger than the values shown in fig. 3 because of the larger defect's effective radius. However, the same qualitative behavior is observed. For small distortions, the elastic response of the CL agrees quantitatively with the JdG model, whereas, for large distortions, a departure from the linear model along with a softening of the CL stiffness is observed. In this case, the degree of non-linearity is found to decrease with the contact angle as well.

**Summary.** – We have used numerical methods to study the equilibrium configurations of a liquid contact

line pinned on a single defect and the corresponding capillary restoring force. Our results show that the decay of the contact line to the unperturbed position is slightly faster than the logarithmic fall-off predicted by the linear elastic model. Furthermore, the restoring force of the contact line exhibits a significant degree of non-linearity, independently of the value the contact angle far from the defect. However, the non-linearity of the contact line elasticity decreases with the contact angle.

Although these results apply to the pinning on a single defect, they may help explain the discrepancy between the roughness exponent of the line measured on heterogeneous surfaces and the value predicted based on the harmonic approximation. Indeed, it is known that large enough non-linear terms of the elastic energy increase the theoretically expected roughness.

Finally, the numerical approach introduced here can be extended straightforwardly to a large variety of heterogeneous surfaces and to axisymmetric drops, thus enabling the study of phenomena such as contact angle hysteresis.

\*\*\*

The author acknowledges valuable discussions with K. BRAKKE. This work is supported by the U.S. DOE under contract No. DE-AC02-98CH10886.

## REFERENCES

- [1] DE GENNES P. G., *Rev. Mod. Phys.*, **57** (1985) 827.
- [2] BLOSSEY R., *Nat. Mater.*, **2** (2003) 301.
- [3] CUI Y., BJÖRK M. T., LIDDLE J. A., SÖNNICHSEN C., BOUSSERT B. and ALIVISATOS A. P., *Nano Lett.*, **4** (2004) 1093.
- [4] JOANNY J. F. and DE GENNES P. G., *J. Chem. Phys.*, **81** (1984) 552.
- [5] MOULINET S., GUTHMANN C. and ROLLEY E., *Eur. Phys. J. E*, **8** (2002) 437.
- [6] ROSSO A. and KRAUTH W., *Phys. Rev. E*, **65** (2002) R025101.
- [7] LE DOUSSAL P., WIESE K. J., RAPHAL E. and GOLESTANIAN R., *Phys. Rev. Lett.*, **96** (2006) 015702.
- [8] BRAKKE K. A., *Exp. Math.*, **1** (1992) 141.
- [9] BRAKKE K. A., *Surface Evolver Manual* ([www.susqu.edu/brakke/evolver/downloads/manual226.pdf](http://www.susqu.edu/brakke/evolver/downloads/manual226.pdf)).
- [10] DARHUBER A. A., TROIAN S. M., MILLER S. M. and WAGNER S., *J. Appl. Phys.*, **87** (2000) 7768.
- [11] GAU H., HERMINGHAUS S., LENZ P. and LIPOWSKY R., *Science*, **283** (1999) 46.
- [12] BRANDON S., WACHS A. and MARMUR A., *J. Colloid Interface Sci.*, **191** (1997) 110.
- [13] NADKARNI G. D. and GAROFF S., *Europhys. Lett.*, **20** (1992) 523.